

# Effects of dipole-dipole interaction between cigar-shaped BECs of cold alkali atoms: Towards inverse-squared interactions

Yue Yu

*Department of Physics and Center for Field Theory and Particle Physics, Fudan University, Shanghai 200433, China and  
The State Key Laboratory of Theoretical Physics, Institute of Theoretical Physics,  
Chinese Academy of Sciences, P.O. Box 2735, Beijing 100190, China*

Zhuxi Luo

*School of Economics, Fudan University, Shanghai 200433, China*

Ziqiang Wang

*Department of Physics, Boston College, Chestnut Hill, MA 02467, USA*

(Dated: April 29, 2022)

We show that the dipole-dipole coupling between Wannier modes in cigar-shaped Bose-Einstein condensates (BECs) is significantly enhanced while the short-range coupling strongly suppressed. As a result, the dipole-dipole interaction can become the dominant interaction between ultracold alkali Bose atoms. In the long length limit of a cigar-shaped BEC, the resulting effective one-dimensional models possess an effective inverse squared interacting potential, the Calogero-Sutherland potential, which plays a fundamental role in many fields of contemporary physics; but its direct experimental realization has been a challenge for a long time. We propose to realize the Calogero-Sutherland model in ultracold alkali Bose atoms and study the effects of the dipole-dipole interaction.

PACS numbers: 67.85.Pq, 37.10.Jk, 11.30.Pb

## I. INTRODUCTION

The quantum simulation of strongly correlated systems with cold atoms and molecules is an advancing subject in modern physics [1]. With precise control of system parameters by external fields, the quantum simulation becomes an ideal method to capture the key physics of such formidable many-body systems. The first example is the simulation, using boson atoms, of the Bose-Hubbard model [1], the most basic and fundamental model of strongly correlated electron materials that remains to be better understood. Other examples of quantum simulation include using fermion atoms to simulate the fermionic Hubbard model [2], polar molecules and Rydberg atoms to simulate various quantum spin and more exotic quantum systems [3, 4].

Among the strongly correlated models of condensed matter and many-body systems, there is an important class of one-dimensional models with inverse-squared interactions. The prototype of the latter is the celebrated Calogero-Sutherland model [5, 6] that nowadays plays a fundamental role in many branches of modern physics [7, 8]. Besides its importance in theoretical and mathematical physics, the Calogero-Sutherland type of models are often applied to explain the physical phenomena in fractional quantum Hall effects [9], quantum exclusion statistics [10], black hole physics [11], quantum spin systems [12], and so on. It is of great interests to directly simulate the Calogero-Sutherland model using ultracold atoms. However, the inverse-squared interaction presents a serious challenge for experimental realizations amid the lack of a concrete proposal.

In this paper, we propose a possible realization of the

Calogero-Sutherland type of models by suppressing the  $s$ -wave interaction while enhancing the dipole-dipole interaction of cold alkali atoms on optical lattices. The dipole-dipole interaction between cold particles [13] is the basis for the cold polar molecular simulator and Rydberg simulator. These cold particle gases usually have strong dipolar couplings [4, 14–17]. For alkali atoms, the effect of the dipole-dipole interaction was thought to be of negligible significance because the dipole-dipole coupling is too weak compared to the  $s$ -wave scattering. However, the cold alkali atom gases are much easier to be made and manipulated, and are far more stable than the polar molecule and dipolar atomic gases.

We study the effective interactions between the single mode fluctuations in an array of cigar-shaped cold alkali atom Bose-Einstein condensates (BECs) which are confined in a one-dimensional optical lattice [18, 19]. Remarkably, we find that the dipole-dipole interaction in these systems reduces to an inverse-squared interaction between the single modes with a significantly enhanced coupling strength proportional to the number of atoms in a single BEC. Moreover, the  $s$ -wave scattering is strongly reduced with the effective short-range interaction strength scaling approximately as the inverse of the number of atoms. As a result, in the limit where the single BEC is long, the effective on-site interaction can be neglected and the system is governed by the dominating inverse-squared interaction, i.e., the Calogero-Sutherland model. The material parameters of the alkali metals will be considered for the feasibility of our proposal of a quantum simulator of the Calogero-Sutherland model to study the dipole-dipole interactions.

This paper was organized as follows: In Sec. II, we

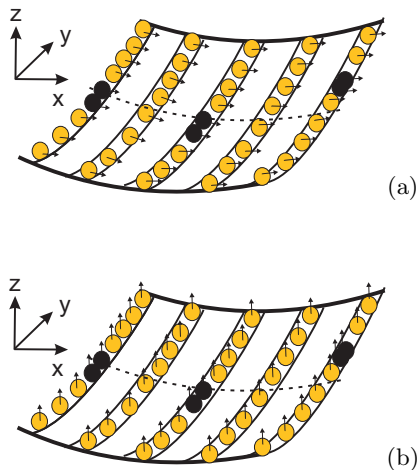


FIG. 1: (color online) The array of cigar-shaped cold atom clouds on an optical lattice. (a) The dipoles are polarized along the  $x$ -direction. (b) The dipoles are polarized along the  $z$ -direction. The yellow spots are the BEC substrate and the black spots are the quasi-atom with the inverse-squared interaction.

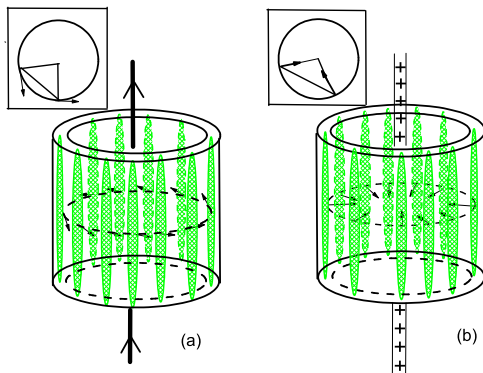


FIG. 2: (color online) Cigar-shaped BEC (green) confined to a cylinder. (a) The magnetic dipoles; (b) The electric dipoles. The inserts indicate the directions of the dipoles.

setup the system we are considering and derive the effective single-band model. In Sec. III, we show that why the inverse-square potential becomes dominant in this system and study the dilute gas limit. The section IV demonstrate the experimental implications. We conclude in Section V.

## II. EFFECTIVE SINGLE-BAND MODEL

### A. Setups of the system

We consider a cold Bose alkali atom cloud with a small dipole moment ( $\sim 1\mu_B$ ). In the presence of a strong

$z$ -direction confinement, the cloud has a pancake shape trapped in the  $x$ - $y$  plane with the trapping frequencies  $\omega_x$  and  $\omega_y$ . The size of the system is therefore  $L_{x,y} = \sqrt{\hbar/m\omega_{x,y}}$ . Using a periodic optical potential along the  $x$ -direction, the pancake is incised into a lattice of cigar-shaped gases. The frequency of the optical potential is denoted as  $\omega_p$ , with the oscillator length satisfying  $\hbar\omega_p = \hbar$ . An applied external field parallel to the  $x$ -axes, or perpendicular to the  $x$ - $y$  plane polarizes all the dipoles along the field direction as shown in Fig.1(a) and (b), respectively. This setup is towards the Calogero model [5].

Another setup follows from rolling the  $x$ - $y$  plane to form the surface of a cylinder as shown in Fig.2. This geometry of the optical lattice is not yet realized. One possibility is using the Laguerre-Gaussian laser beams, which have been applied or proposed to build many periodic optical lattices, e.g., the circular lattice [23], the ring lattice [24], and even a possible torical lattice [25]. However, there are many technical difficulties and complication need to be engineered. It will not be the main focus of this work. Sutherland's periodic variant [6] can be realized with this setup.

### B. Derivation of an effective single-band model

We first focus on the setup shown in Fig. 1 and set  $\omega_x = 0$ . The energy scale in the problem is

$$\hbar\omega_y \ll k_B T \ll \hbar\omega_p.$$

Thus, we are faced with a multi-band problem. Following the two-step procedure proposed in [19], we aim to reduce the multi-band problem to an effective single-band one. First, we treat a single cigar-shaped gas on a given lattice site. The lowest energy level is a BEC and higher levels correspond to the thermal cloud. Denote on every site the wave function of a whole cigar-shaped BEC  $\Psi_0(y)$ , and the number of BEC atoms on each site  $N_0$ . In addition, the condensate size is marked as  $R_y$  on each site. The equation of state with only short-range interactions has been solved exactly in the weak interaction limit [18]. It was shown that even in the presence of phase fluctuations (collective modes), the atom number in a BEC can be determined at any given temperature [19]. For atoms carrying a dipole, in addition to the short-range interaction, there is a dipole-dipole interaction potential

$$V_d(\mathbf{r}, \mathbf{r}') = \frac{\mathbf{d} \cdot \mathbf{d}' - 3(\mathbf{d} \cdot \hat{\mathbf{R}})(\mathbf{d}' \cdot \hat{\mathbf{R}})}{R^3}, \quad (1)$$

where  $\mathbf{R} = \mathbf{r} - \mathbf{r}'$  and  $\hat{\mathbf{R}} = \mathbf{R}/R$ ;  $\mathbf{d}$  and  $\mathbf{d}'$  are the dipole moments of the atoms located at  $\mathbf{r}$  and  $\mathbf{r}'$ , respectively. We consider all  $\mathbf{d}$  to be parallel as shown in Fig. 1. The Fourier components of the dipolar interacting potential do not contain any singularity in momentum space other than providing an anisotropic term. Therefore, for a cold atom gas with weak dipolar interactions, this anisotropy

does not cause a qualitative difference and we can continue to use the method given in Ref. [18] to solve the equation of state and determine the atom number  $N_0(T)$  in a BEC.

The second step is to consider the coupling between sites [19]. If  $\hbar\omega_y \ll N_y U_0 \ll \hbar\omega_p$ , where  $N_y$  is the average atom number in a cigar-shaped gas (including those in thermal cloud) and  $U_0$  the on-site repulsion, the wave function may be approximated by the product of the single atom ground state wave function in the  $x$ -direction and the cigar-shaped atom gas in the  $y$  direction. Notice that because we have a BEC  $\Psi_0(y)$  at every site and obviously  $N_0 \lesssim N_y$ , the coupling between the sites will be dominated by tunneling from a BEC to a condensate as opposed to a thermal cloud. As a result, this multi-band problem can be reduced to a single band one [19], i.e., the field operator can be approximated by

$$\psi(\mathbf{r}) \approx \sum_i a_i w(x - x_i) \Psi_0(y),$$

where the bosonic mode  $a_i$  corresponds to annihilating a quasi-atom mode described by the product of the Wannier function  $w(x)$  and the cigar-shaped BEC wave function  $\Psi_0(y)$ . Under this approximation, we arrive at an effective single band boson model with renormalized on-site and renormalized dipole-dipole interactions [19].

### III. THE LATTICE MODEL WITH INVERSE-SQUARED INTERACTION

#### A. Inverse-squared Interaction

Keeping only the nearest neighbor hopping and expanding the on-site energy to the second order near the average occupation  $N_0$  [19, 20], we obtain the effective single-band lattice model described by the Hamiltonian,

$$H = - \sum_{\langle ij \rangle} t a_i^\dagger a_j + \frac{U_R}{2} \sum_i \delta n_i (\delta n_i - 1) + \sum_{i < j} U_{d,ij} \delta n_i \delta n_j, \quad (2)$$

where  $\delta n_i = a_i^\dagger a_i - N_0$  is the deviation of the atom number from the average number per site;  $t$  is the nearest neighbor hopping amplitude. We emphasize that here the hopping 'particle' is not the whole cigar-shaped BEC as a 'giant particle' but only the particle number variance between the adjacent lattice sites. We define the original bare on-site repulsion as

$$U_0 = \frac{4\pi\hbar^2 a}{m} \int dx dy dz |\psi_0(z)|^4 |w(x)|^4 |\psi_0(y)|^4$$

where and  $a$  is the  $s$ -wave scattering length,  $\psi_0(z)$  is the perpendicular confined single particle wave function and  $\psi_0(y)$  is the single particle wave function in the  $y$ -direction.

The renormalized on-site potential  $U_R$  due to the condensation of atoms in the  $y$ -direction is *not simply* given by replacing  $\psi_0(y)$  in  $U_0$  by  $\Psi_0(y)$ , the condensate wave function. Because the condensed wave function is spread out by the on-site repulsion,  $U_R$  is defined by [19]

$$U_R = \frac{\partial^2 F}{\partial N_0^2}, \quad (3)$$

where  $F$  is on-site free energy given by [20]

$$F = F_{TF} + \int dx w^*(x) (-\hbar^2 \frac{d^2}{dx^2} + V(x)) w(x). \quad (4)$$

The Thomas-Fermi free energy  $F_{TF}$  is the Gross-Pitaevskii energy of the  $y$ -direction one-dimensional BEC in which the dipole-dipole interaction within the single BEC is considered.

The ratio between  $U_R$  and  $U_0$  without dipole-dipole interaction has been estimated in Ref. [19],  $U_R = U_0 \frac{l_p}{R_y}$ , where  $R_y$  is the Thomas-Fermi radius of the cigar-shaped BEC in the  $y$ -direction and  $l_p$  is the lattice spacing under the consistency condition

$$L_y/a \ll N_0 \ll (\hbar\omega_p/\hbar\omega_y)^2 \sqrt{2\pi} l_p/a.$$

Hereafter, we set  $l_p = 1$  as the unit of length unless stated explicitly. The bare on-site interaction is strongly renormalized because the on-site wave function spreads out the BEC wave function [19].

For alkali atoms we are studied, the bare dipole-dipole interaction in a single cigar-like BEC is very weak comparing to  $U_0$ . Therefore, we can take  $U_R \sim U_0 \frac{l_p}{R_y}$  as a good approximation. The only change is the Thomas-Fermi radius  $R_y$  which is determined when the dipole-dipole interaction between the atoms within the single BEC is included.

The hopping amplitude  $t$ , as pointed out by Refs. [19, 20], is almost not renormalized because the transverse Wannier function  $w(x)$  is almost not affected by the spread-out of the BEC wave function.

The last term in Eq. (2) is the renormalized dipolar interaction potential between the fluctuating modes of different cigar-like condensates ( $i < j$ ). This is given by

$$U_{d,ij} = \int d\mathbf{r} d\mathbf{r}' |w(x - x_i)|^2 |w(x' - x_j)|^2 V_d(\mathbf{r}, \mathbf{r}') |\Psi_0(y)|^2 |\Psi_0(y')|^2. \quad (5)$$

Consider the case where the condensate size  $R_y$  is much larger than the lattice size  $L_x$ , i.e.  $R_y \gg L_x$ . We approximate the BEC wave function by the average density of atoms in a single BEC,  $|\Psi_0(y)|^2 \approx N_0/R_y$ . Under this condition, it is easy to carry out the integration over  $y$  and  $y'$  and arrive at

$$U_{d,ij} \approx \int dx dx' |w(x - x_i)|^2 |w(x' - x_j)|^2 \times \frac{GR_y}{(x - x')^2 \sqrt{(x - x')^2 + R_y^2}} \approx \frac{G}{(x_i - x_j)^2} + O\left(\frac{1}{R_y^2}\right), \quad (6)$$

where  $G = -2d^2N_0^2/R_y$  for the setup shown Fig. 1(a) and  $G = 2d^2N_0^2/R_y$  for the setup in Fig. 1(b). Thus, we have obtained a one-dimensional lattice model with on-site and inverse-squared interactions between the single modes in the ground state. The finite size effect of the cigar-shaped BEC only contributes a negligible  $O(1/R_y^2)$  correction. We observe that while the on-site coupling constant in one dimension is reduced a factor  $l_p/R_y$ , the long range interacting coupling is renormalized by an additional factor  $2N_0^2$  besides the reduced factor  $l_p/R_y$ . If  $N_0^2 \gg R_y/l_p$ , the latter can be remarkably enhanced.

### B. Dominance of the renormalized dipole-dipole interaction

The stability condition of a single BEC at a given site is governed by the ratio of dipolar to on-site interactions  $\epsilon_{dd} = d^2/(3U_0) < 1$  [21], where  $d$  is the magnitude of the dipole moment. For alkali metal atoms,  $d \sim 1\mu_B$  and  $\epsilon_{dd} \ll 1$ . For example,  $\epsilon_{dd} = 0.007$  for  $^{87}\text{Rb}$ . In the present context, while the renormalized on-site interaction  $U_R$  is reduced by a factor  $\frac{l_p}{R_y}$  from  $U_0$  [19], our results show that the effective dipole moment is enhanced to  $d_R = dN_0$  as shown in Eq. (6). Therefore, although the bare ratio  $\epsilon_{dd} \ll 1$ , the renormalized on-site interaction can be negligibly weak compared to the renormalized dipole-dipole interaction in the effective one-dimensional single-band model. Indeed, it is instructive to introduce a renormalized ratio of dipolar and on-site interactions,  $\epsilon_{d_R d_R} = d_R^2/(3U_R) = \epsilon_{dd}N_0^2R_y/l_p$ . The latter that can be much larger than unity. Assuming  $N_0 \sim 10^3$  and  $R_y/l_p \sim 10^3$ , we estimate that  $\epsilon_{d_R d_R} \gtrsim 10^6$  for  $^{87}\text{Rb}$ .

### C. Trapping potential in the $x$ -direction

We have obtained a homogeneous lattice boson model with inverse-squared interaction by neglecting the trapping in the  $x$ -direction. Putting back the harmonic trap with the frequency  $\omega_x$  may affect the atom number  $N_0(x)$  at each site. If the width of a single BEC is too wide, the number of atoms per site may vary from site to site and  $N_0$  in the center of trapping potential can be several times that far away from the center. However, within a cigar-shaped dipolar BEC, the dipole-dipole repulsion is strong enough against increasing the width of the single BEC at the trapping center. Therefore, the factorization of the ground state wave function is still valid and  $N_0$  remains approximately a constant. The resulting inhomogeneous model is given by  $H$  in (2) augmented by an additional term  $\sum_i V_{h,i}\delta n_i$ , where

$$V_{h,i} = \frac{1}{2}m\omega_x^2 \int dx |w(x - x_i)|^2 x^2 \quad (7)$$

is the harmonic trapping potential along the  $x$ -direction.

### D. Dilute gas limit and the Calogero-Sutherland model

Denoting the total fluctuations in the atom number as  $\delta N = \sum_i \delta n_i$ . The fixed number of  $\delta N$ -particle system may be described by a continuum model in the dilute gas limit with  $\delta N/L_x \ll 1$ , where the dispersion  $-t \cos k/\hbar \sim k^2/(2m_R)$  with the effective mass  $m_R \sim \hbar^2/t$ . Dropping the negligible on-site interaction as argued above, the effective Hamiltonian reads

$$H_{CS} = \sum_{i=1}^{\delta N} \left( -\frac{\hbar^2}{2m_R} \frac{d^2}{dx_i^2} + \frac{m_R \omega_R^2}{2} x_i^2 \right) + \sum_{i < j} \frac{G}{|x_{ij}|^2}, \quad (8)$$

where  $x_{ij} = x_j - x_i$  and the effective trapping potential is defined via  $m\omega_x^2 = m_R\omega_R^2$ . The model described by the Hamiltonian (8) is precisely the celebrated Calogero-Sutherland model [5, 6]. A bosonic ‘‘particle’’ at  $x_i$  in this continuum model corresponds to one more atom than  $N_0$  at site  $i$  in the lattice model. The ground state wave function is given by

$$\Psi_{0,\lambda}(x_1, \dots, x_{\delta N}) = \prod_{1 \leq j < k \leq \delta N} |x_{jk}|^\lambda e^{-\frac{m_R \omega_R}{2\hbar} \sum_j x_j^2} \quad (9)$$

with the ground state energy  $E_g = \frac{1}{2}\delta N \hbar \omega_R (\lambda(\delta N - 1) + 1)$ . Here,  $\lambda = \lambda_\pm = \frac{1 \pm \sqrt{1+4g}}{2}$  are the solutions of the equation  $\lambda(\lambda - 1) = g = (m_R/\hbar^2)G$ . For a weak on-site interaction with  $U_0/t < 1$ ,  $g$  may vary as  $t$ . If  $l_p/R_y \sim O(10^{-3})$ ,  $N_0 \sim O(10^3)$ ,  $U_0/t \sim O(10^{-1})$ , the absolute value of  $g$  is of the order unity. For example, for the repulsive interacting  $^{87}\text{Rb}$  atoms, we estimate  $g \approx 0.021N_0^2U_0/tR_y \sim 2.1$  [26]. The exact solution of the Calogero-Sutherland model can now be utilized to make predictions for the stability of the ultracold alkali atoms.

For the setups in Fig. 1(a),  $g < 0$ . If  $g < -1/4$ ,  $\lambda$  becomes imaginary. This leads to an imaginary ground state energy and the system is unstable. However, when  $-1/4 \leq g < 0$ , the ground state is stable for  $0 \leq \lambda_- < 1/2$  despite of the attractive interaction.

For the setups in Fig. 1(b),  $g > 0$ . For  $-1/2 < \lambda_- < 0$ , i.e.,  $g < \frac{3}{4}$ , the wave function is still square integrable. This implies that the system will also be unstable if the repulsion between particles is not strong enough. On the other hand, for  $g > \frac{3}{4}$ , (9) with  $\lambda = \lambda_- < -1/2$  is not a physical solution because it is not square integrable. A physically stable solution is given by (9) with  $\lambda = \lambda_+$ .

We next consider the geometry in Fig. 2. In this geometry, the cylinder extends along the  $y$ -direction and circulates in the  $x$ -direction. For  $R_y \gg L_x$ , one may prove that, up to a constant term, the renormalized dipole-dipole interaction is a periodic inverse-squared interaction as in the Sutherland model [6]

$$V \approx \pm \sum_{i \neq j} \frac{\pi^2 \lambda(\lambda - 1)}{L_x^2 \sin^2[\pi x_{ij}/L_x]} + O\left(\frac{1}{R_y^2}\right),$$

where  $\pm$  are corresponding to Fig. 2(a) and Fig. 2(b), respectively. The similar but periodic solutions were obtained by Sutherland [6].

#### IV. EXPERIMENTAL IMPLICATIONS

The first prediction on the effects of the dipole-dipole interaction between the alkali atoms is unstable when  $g < -1/4$ . The Calogero-Sutherland gas collapses the single modes to a single lattice site (a given single cigar-shaped BEC) when  $g < -1/4$  for the setups in Fig. 1(a) and 2(a) and  $g < 3/4$  for the setups of Figs. 1(b) and 2(b). Although in practice it is impossible that the lattice gas collapses to a single site, this means the one-dimensional lattice gas with dipole-dipole interaction becomes unstable to tend to the center of the lattice. We are unable to estimate the details of this tendency. The time-of-flight experiments measure the momentum distribution of the trapped cloud [22]. In these experiments, the predicted tendency can be observed and regarded as a ubiquitous evidence of the effect of the renormalized dipole-dipole interaction.

##### A. Calculation of the momentum distribution

One can study these effects more quantitatively. For example, one can consider the long wave length limit of the Green's function at a given time in the Sutherland model, which is given by [27]

$$G(x, 0) \propto 1 + 2 \sum_{\ell=1}^{\infty} (-1)^{\ell} B_{\ell} \frac{\cos 2\ell k_F x}{|2k_F x|^{2\ell^2/\lambda}} \quad (10)$$

where  $B_{\ell}$  are regularization-dependent constants and  $k_F = \pi\delta N/L_x$  is the effective Fermi momentum. This corresponds to the infinite mass or localized limit. The momentum distribution is the Fourier transformation of this Green's function. For the lowest energy sector with  $\ell = 1$ , the momentum distribution in the small  $k$  and large  $k$  limits are approximated by [27]

$$\begin{aligned} n_k &\propto |k|^{\lambda/2-1} \text{ if } |k| \ll k_F, \\ &\propto |k|^{-2\lambda-2} \text{ if } |k| \gg k_F. \end{aligned} \quad (11)$$

We see that when  $\lambda < 2$ , the system is in a quasi-condensed state. When  $\lambda > 2$ , the momentum distribution vanishes as a power law for small  $k$ , which is the Luttinger liquid behavior for bosons. At the critical point,  $\lambda = 2$ , a logarithmic divergence arises, i.e.,  $n_k = (1/2) \ln(2k_F/|k|)$  for  $|k| < 2k_F$  and  $n_k = 0$  for  $|k| \geq 2k_F$  [6]. These momentum distributions have been shown in Ref. [27] and we display them schematically in Fig. 3(a).

Eq. (11) calculated by the Sutherland model is also valid for the Calogero model because the result is only dependent on  $k_F$ .

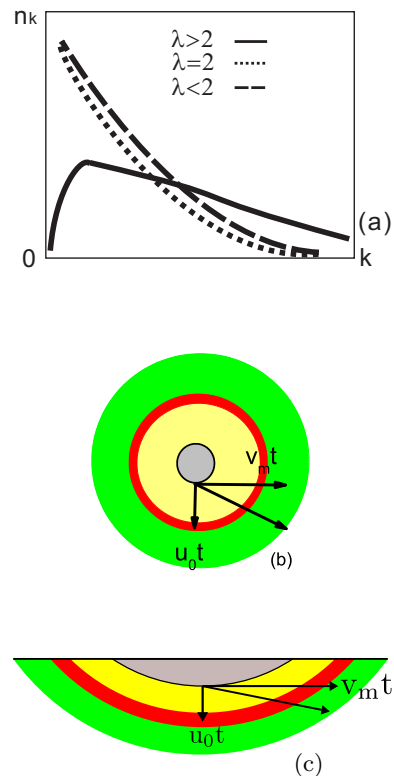


FIG. 3: (color online) (a) The schematic diagram of the momentum distribution. (b) The top-view of the time-of-flight image. The grey area is the original cylinder. The yellow regime only has very few atoms. Most of the atoms arrive at time  $t$  in the red area and the green region describe the arrival of those atoms with the momentum distribution in Eq. (11). (c) The parabolic counterpart of (b).

##### B. Experimental proposal measuring $n_k$

The projected density profile in the plane perpendicular to the  $y$ -axis directly reflects the momentum distribution  $n_k$  since the momentum along the circle of the setup Fig. 2 is a good quantum number. The quasi-condensate is not easy to be distinguished from the case without the dipolar interaction. However, for  $\lambda > 2$ , when we switch off all traps but the inner wall of the cylinder, the cloud along the radial direction expands much faster than that along the axial and tangent directions because it is the most squeezed along this direction owing to a larger zero point energy. Denote  $u_0$  as the velocity of the radial motion of a single cigar-shaped cloud and  $v_m$  as the fastest velocity of the particles along the circle, the top view of the cylinder during a time-of-flight experiment is shown in Fig. 3(b). At time  $t$  after turning off the traps, most of the background BEC atoms arrive at the red area while the unconventional momentum distribution in Eq. (11) can be measured by studying the atoms arriving in the green region.

As the setup Fig. 2 is not realized in the existent experiments, we would like to point out that the similar measurement can also be done for the setup Fig. 1. As

we augured, Eq. (11) still hold for the Calogero model. Because of the existence of the trapping potential, the time-of-flight process now has a parabolic profile instead of the circular profile. (See Fig. 3(c).) When all the traps are removed, we add a potential above the  $z = 0$  plane which plays the role of the inner wall potential in Fig. 1 so that the atoms cannot fly upward. The speed  $v_m$  of the atoms flying to the green area is great than  $u_0$ . Therefore, the density profile in the green area reflects the momentum distribution in Eq. (11) with  $|k| \gg k_F$ , i.e.,  $n_k \propto |k|^{-2\lambda-2}$ .

We note that although Eq. (11) provides qualitatively correct results, more quantitative description of the experimental data can be obtained by calculating the Green's function (10) and the momentum distribution (11) in terms of the lattice model (2).

## V. CONCLUSIONS

In conclusion, we have shown that the dipole-dipole interaction between the Wannier modes of cigar-shaped

BECs is strongly enhanced and governed by an inverse-squared potential that dominates over the downward-renormalized short-range interaction. Based on this finding, we put forth a concrete proposal to use ultracold alkali atoms on optical lattices as a quantum simulator to realize the celebrated Calogero-Sutherland model, which in turn provides insights and predictions to help understand the unconventional many-body effects in these systems.

## ACKNOWLEDGEMENT

The authors thank Yingmei Liu, Kun Yang, Su Yi and Li You for useful discussions. This work was supported by (2012CB821402, 2009CB929101), NNSF of China (11174298,11121403), and DOE grants DE-FG02-99ER45747 and DE-SC0002554.

- 
- [1] D. Jaksch, C. Bruder, J. I. Cirac, C. W. Gardiner, P. Zoller, Phys. Rev. Lett. **81**, 3108 (1998).
  - [2] See D. Jaksch and P. Zoller, Ann. Phys. **315**, 52 (2005).
  - [3] A. Micheli, G.K. Brennen, P. Zoller, Nature Phys. **2**, 341 (2006).
  - [4] H. Weimer, Markus Müller, I. Lesanovsky, P. Zoller, and H. P. Bchler, Nature Phys. **6**, 382 (2010).
  - [5] F. Calogero, J. Math. Phys. **10**, 2191 and 2197 (1969).
  - [6] B. Sutherland, J. Math. Phys. **12**, 246 (1971); Phys. Rev. A **4**, 2019 (1971); **5**, 1372 (1972).
  - [7] See e.g., J. F. van Diejen and L. Vinet (Eds.), *Calogero-Moser-Sutherland Models: CRM Series in Math. Phys. 2000 XXV*, (Springer, Berlin, Heidelberg, New York 2000) and references therein.
  - [8] A. P. Polychronakos, J. Phys. A **39**, 12793 (2006).
  - [9] Y. Yu, W. J. Zheng and Z. Y. Zhu, Phys. Rev. B **56**, 13279 (1997)
  - [10] D. Bernard and Y. S. Wu, in Proc. 6th Nankai Workshop, eds. M. L. Ge and Y. S. Wu, World Scientific (1995).
  - [11] G. W. Gibbons and P. K. Townsend, Phys. Lett. B **454** 187 (1999).
  - [12] F. D. M. Haldane, Phys. Rev. Lett. **60**, 635 (1988); B. S. Shastry, Phys. Rev. Lett. **60** 639 (1988).
  - [13] S. Yi and L. You, Phys. Rev. A **61**, 041604(R) (2000).
  - [14] J. Doyle, B. Friedrich, R. V. Krems and F. Masnou-Seeuws, Eur. Phys. J. D **31**, 149 (2004).
  - [15] A. Griesmaier, J. Stuhler, T. Koch, M. Fattori, T. Pfau, and S. Giovanazzi, Phys. Rev. Lett. **94**, 160401(2005).
  - [16] K. Aikawa, A. Frisch, M. Mark, S. Baier, A. Rietzler, R. Grimm, and F. Ferlaino, Phys. Rev. Lett. **108**, 210401 (2012).
  - [17] M. Lu, N. Q. Burdick, S. H. Youn, and B. L. Lev, Phys. Rev. Lett. **107**, 190401(2011).
  - [18] J. O. Andersen, U. Al Khawaja, and H. T. C. Stoof, Phys. Rev. Lett. **88**, 070407 (2002).
  - [19] D. van Oosten, P. van der Straten, and H. T. C. Stoof, Phys. Rev. A **67**, 033606 (2003).
  - [20] J. B. Li, Y. Yu, A. M. Dudarev and Q. Niu, New J. Phys. **8**, 154 (2006).
  - [21] S. Yi and L. You, Phys. Rev. A **63**, 053607 (2001).
  - [22] W. Ketterle, D. S. Durfee, and D. M. Stamper-Kurn, Proceedings of the International School of Physics 'Enrico Fermi', Course CXL, edited by M. Inguscio et al (IOP Press, Amsterdam, 1999).
  - [23] H.L. Haroutyunyan, G. Nienhuis, Phys. Rev. A **70** (2004) 063408.
  - [24] L. Amico, A. Osterloh, F. Cataliotti, Phys. Rev. Lett. **95**, (2005) 063201. S. Franke-Arnold, J. Leach, M.J. Padgett, V.E. Lembessis, D. Ellinas, A.J. Wright, J.M. Girkin, P. O hberg, A.S. Arnold, Optics Express **15**, 8619 (2007).
  - [25] E.M. Wright, J. Arlt, K. Dholakia, Phys. Rev. A **63**, (2001) 013608. J. Arlt, T. Hitomi, K. Dholakia, Appl. Phys. B **71**, (2000) 549.
  - [26] If we take the laser beam wave length  $\lambda \sim 850\text{nm}$ , which gives the lattice spacing  $l_p = \lambda/2 \sim 425\text{nm}$ . This yields the tunneling amplitude  $t \sim 0.015E_R$  where  $E_R$  is the recoil energy of the atom. This is quite reasonable for a weak interacting optical lattice atom gas. On the other hand,  $R_y \sim 10^2 \mu\text{m}$ . The order estimate  $l_p/R_y \sim O(10^{-3})$  is reachable.
  - [27] G. E. Astrakharchik, D. M. Gangardt, Yu. E. Lozovik, and I. A. Sorokin, Phys. Rev. B **74**, 021105 (2006).